

Supplementary information

22.43%-efficiency flexible modification-free perovskite solar cells with a uniform and anti-reflective ITO/SiO₂/PET/SiO₂ substrate

Jiwen Chen,^{a,b,‡} Xi Fan,^{*b,‡} Jia Li,^b Jinzhao Wang,^c Jixi Zeng,^b Wenqing Zhu^{*a} and Weijie Song^{*b,c,d}

^aSchool of Materials Science and Engineering, Shanghai University, 99 Shangda Road, Shanghai 200444, P.R. China.

^bNingbo Institute of Materials Technology and Engineering, Chinese Academy of Sciences, Ningbo, 315201, P.R. China.

^cCenter of Materials Science and Optoelectronics Engineering, University of Chinese Academy of Sciences, Beijing 100049, P.R. China.

^dResearch Center for Sensing Materials and Devices, Zhejiang Lab, Hangzhou, Zhejiang 311121, P.R. China.

^eSchool of Material Science and Engineering, Hubei University, Wuhan 430062, P.R. China.

*Correspondence: fanxi@nimte.ac.cn (X. F.); wqzhu@shu.edu.cn (W. Z.); weijiesong@nimte.ac.cn (W.J. S.)

‡ Jiwen Chen and Xi Fan contributed equally to this work.

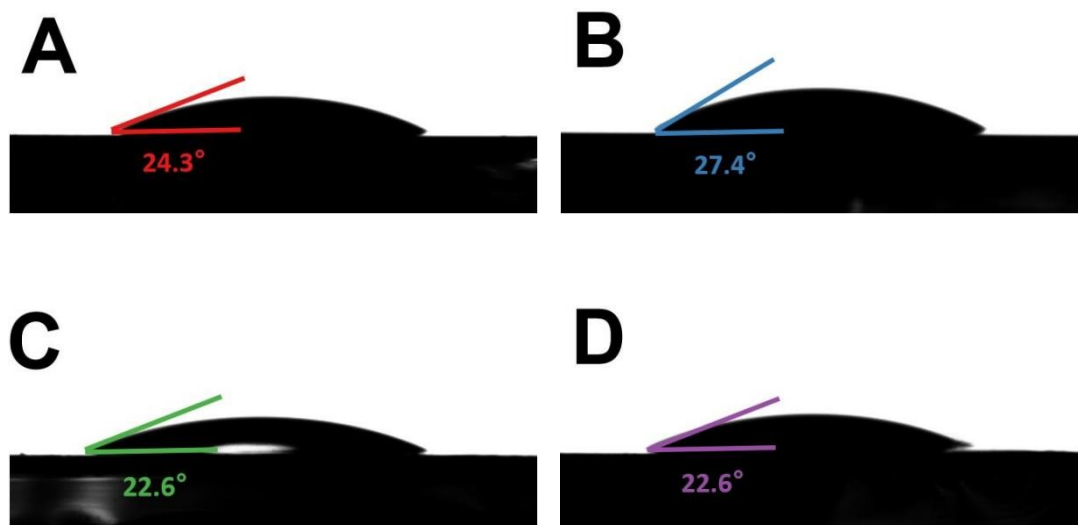


Figure 1. Wettability characteristics of the MeO-2PACz droplets on these ITO transparent electrodes. Obviously, the droplets of MeO-2PACz showed a good wettability with a contact angle of $\sim 24.3^\circ$ on the surfaces of the α -ITO/SiO₂/PET/SiO₂, which is smaller than that ($\sim 27.4^\circ$) of the droplets on the surface of the β -ITO/SiO₂/PET/SiO₂. The smaller contact angle suggests a higher hydrophilic property of the α -ITO and an intimate contact at interfaces. The enhanced wettability is favorable for a better deposition of the MeO-2PACz HTLs. When the MeO-2PACz droplets were dipped on both γ - and δ -ITO, the droplets showed a comparable wettability with a small contact angle of $\sim 22.6^\circ$. The results demonstrate an intimate interface contact between the MeO-2PACz and the γ - and δ -ITO electrodes.

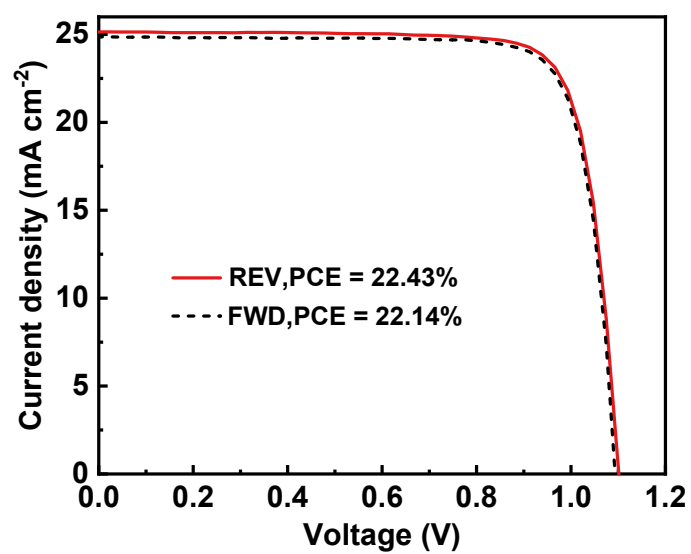


Figure S2. J - V curves of the best flexible unmodified PSCs *via* a forward (FWD) scanning and the reverse (REV) scanning.

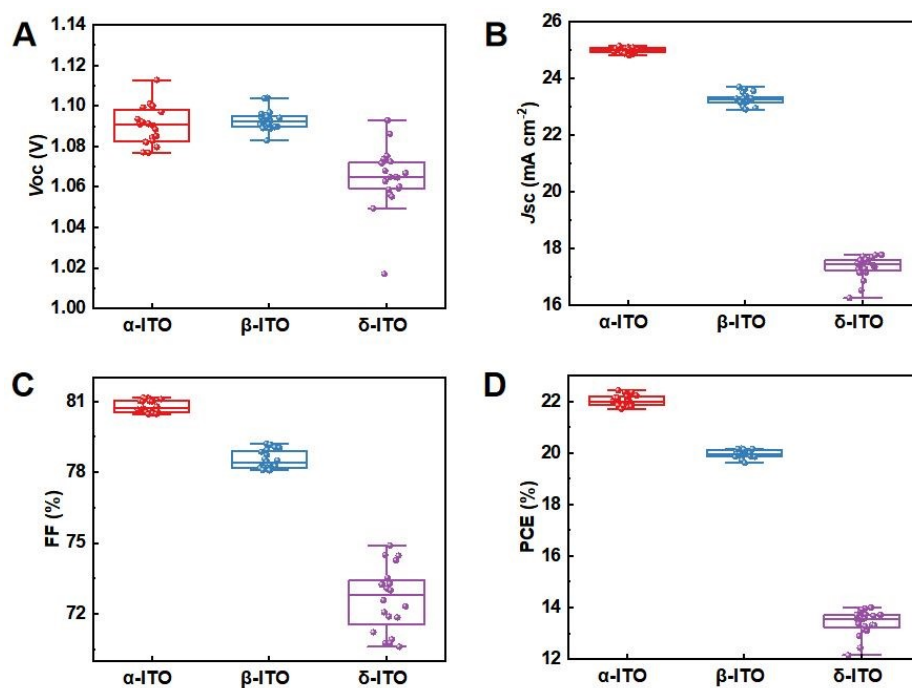


Figure S3. Performance distributions of the flexible PSCs with the different ITO-coated plastic substrates. A) V_{OC} , B) J_{SC} ; C) FF, and D) PCE.

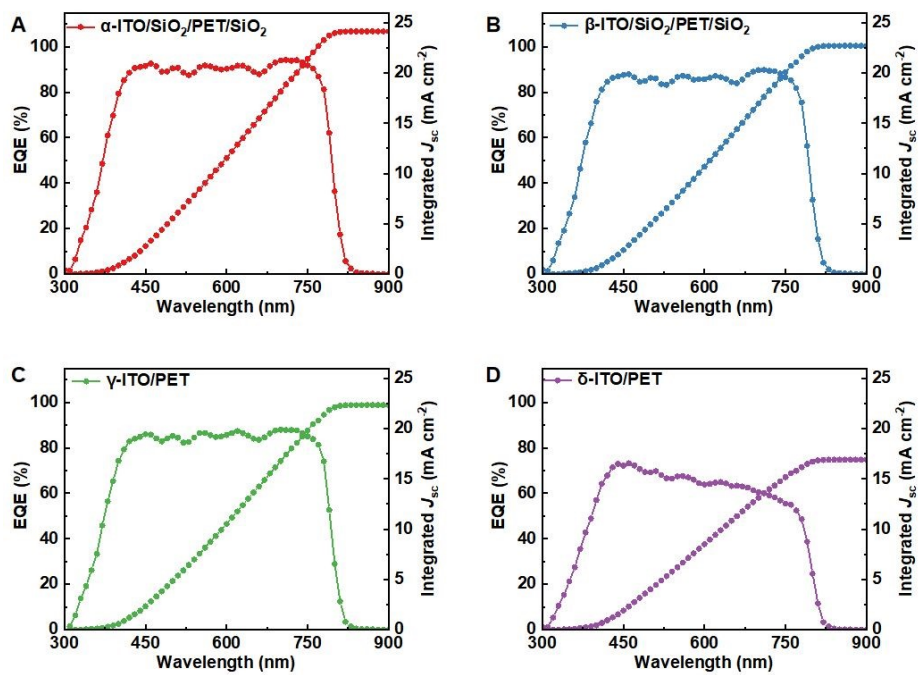


Figure S4. EQE spectra of the flexible PSCs with the different ITO-coated plastic substrates.

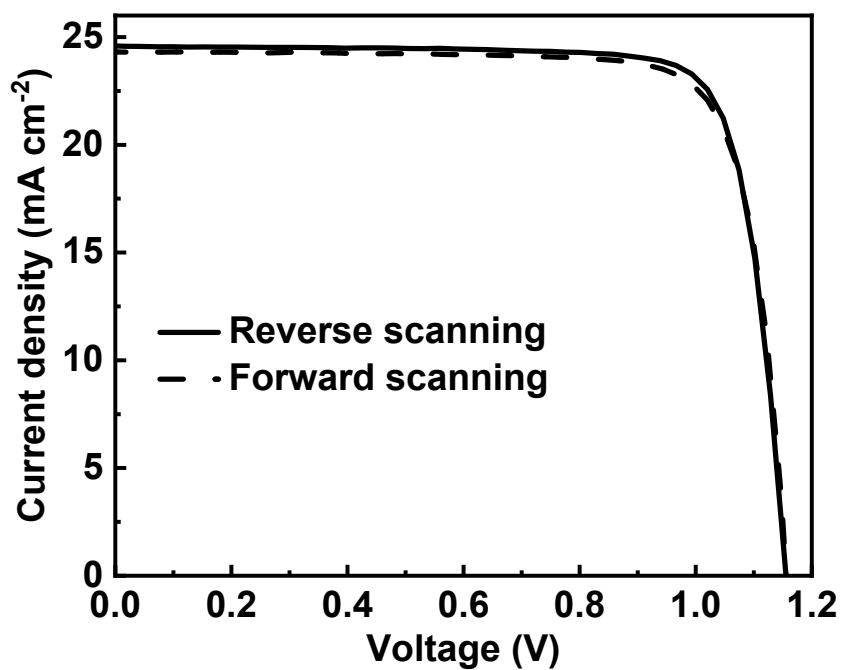


Figure S5. J - V curves of the best flexible GBAC doped PSCs *via* forward scanning and reverse scanning.

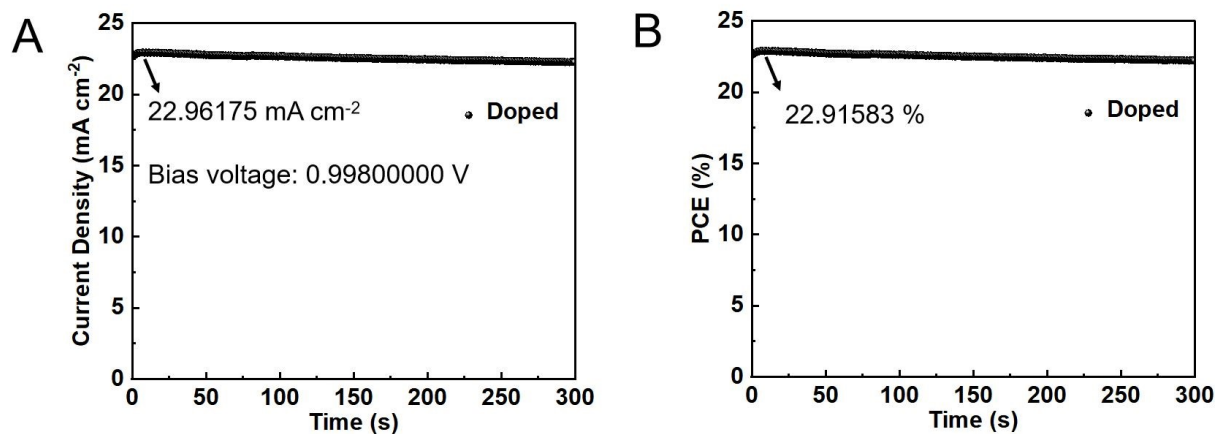


Figure S6. Steady-state photocurrent and power output of the GBAc doped flexible PSCs with the α -ITO/SiO₂/PET/SiO₂.

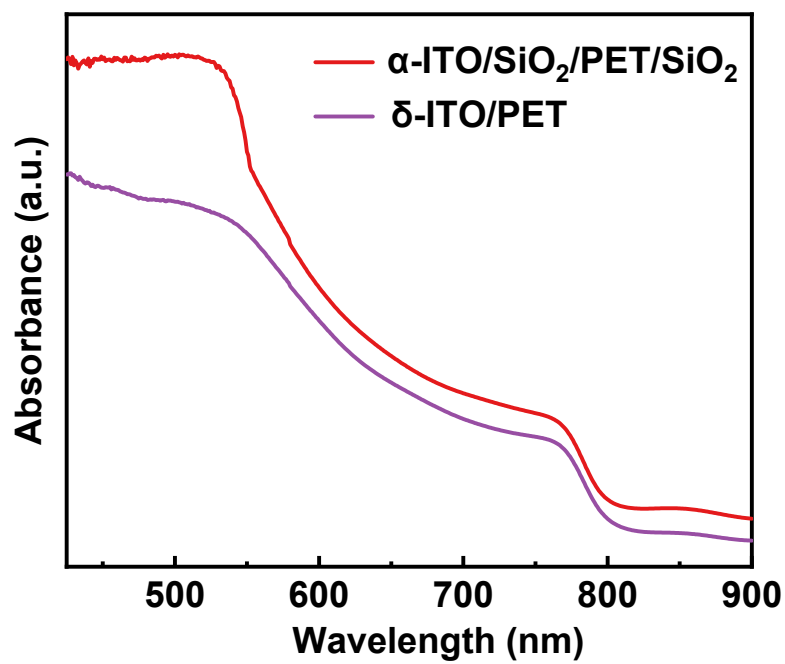


Figure S7. The absorption spectra of the α - and δ -ITO based flexible devices without Ag metals.

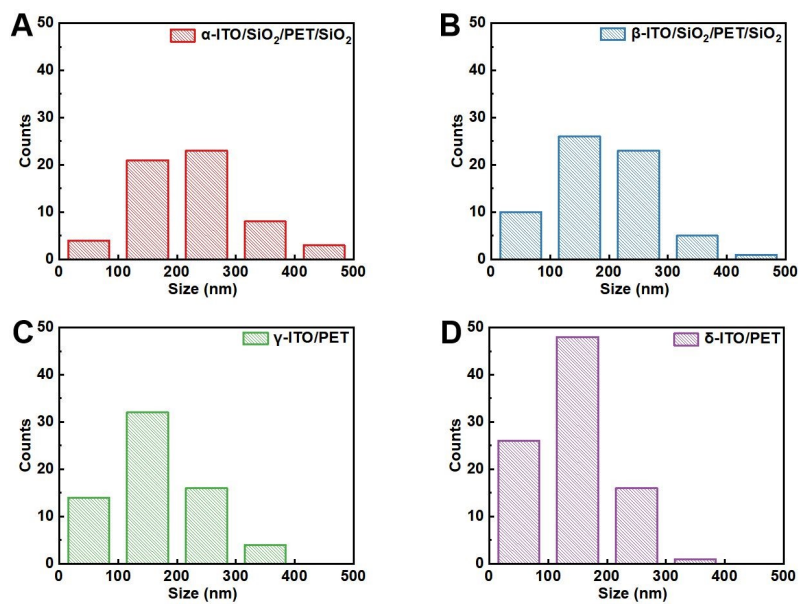


Figure S8. The grain size distribution data of the perovskites on the different ITO-coated plastic substrates.

Table S1. Comparison of the PCEs of the processing-simple flexible PSCs without surface modifications and dopant incorporation.

| Device Structure | V_{OC} [V] | J_{SC} [mA cm ⁻²] | FF [%] | PCE [%] | Refer. |
|---|-----------------|------------------------------------|-----------|--------------|-------------|
| SiO ₂ /PET/SiO ₂ /ITO/MeO- | 1.10 | 25.14 | 81.16 | 22.43 | Here |
| 2PACz/Cs _{0.05} (FA _{0.98} MA _{0.02}) _{0.95} Pb(I _{0.98} Br _{0.02}) ₃ /C ₆₀ /BCP/Ag | 1.10 | 24.24 | 79.45 | 21.11 | 1 |
| PET/ITO/D CPA/Cs _{0.05} (FA _{0.98} MA _{0.02}) _{0.95} Pb(I _{0.98} Br _{0.02}) ₃ /C ₆₀ /BCP/Ag | 1.10 | 24.95 | 76.38 | 20.96 | 2 |
| PET/PEDOT:PSS/PTAA/Cs _{0.05} (FA _{0.95} MA _{0.05}) _{0.95} Pb(I _{0.95} Br _{0.05}) ₃ /PCBM/BCP/Ag | 1.12 | 24.90 | 76.00 | 21.13 | 3 |
| PEN/ITO/PTAA//FA _y MA _{1-y} PbI _{3-x} Cl _x /C ₆₀ /BCP/Cu | 1.05 | 21.86 | 77.42 | 17.77 | 4 |
| SUPA/PEN/ITO/PTAA/MA _{0.6} FA _{0.4} PbI _{2.9} Br _{0.1} /C ₆₀ /BCP/Cu | 1.07 | 21.92 | 80.20 | 18.84 | 5 |
| PEN/ITO/UV-NiO _x /Cs _{0.05} FA _{0.85} MA _{0.1} PbI _{2.91} Br _{0.09} /C ₆₀ /BCP/Cu | 1.11 | 22.26 | 79.57 | 19.70 | 6 |
| PEN/ITO/PTAA/Cs _{0.15} FA _{0.85} Pb(I _{0.95} Br _{0.05}) ₃ /PCBM/BCP/Ag | 1.15 | 22.55 | 80.50 | 20.90 | 7 |
| PET/ITO/PTAA/MAPbI ₃ /C ₆₀ /BCP/Cu | 1.16 | 21.98 | 79.11 | 20.17 | 8 |
| PEN/ITO/NiO _x /Cs _{0.1} FA _{0.7} MA _{0.2} PbI _x Br _{3-x} /PCBM/BCP/Ag | 1.09 | 22.09 | 79.28 | 19.01 | 9 |
| PEN/ITO/Cs _{0.3} (MA _{0.05} FA _{0.95}) _{0.97} Pb(I _{0.95} Br _{0.05}) ₃ /C ₆₀ /BCP/Cu | 1.07 | 23.22 | 74.90 | 18.59 | 10 |
| PET/ITO/PTAA/MAPbI ₃ /C ₆₀ /BCP/Ag | 1.07 | 22.40 | 72.00 | 17.27 | 11 |
| PEN/ITO/PTAA/Cs _{0.05} FA _{0.7} MA _{0.25} Pb(I _{0.93} Br _{0.07}) ₃ /PCBM/BCP/Ag | 1.04 | 23.89 | 74.50 | 18.51 | 12 |
| PEN/ITO/Spiro-TTBb/MAPbI ₃ /PCBM/BCP/Ag | 1.10 | 21.70 | 81.19 | 19.34 | 13 |
| PEN/ITO/NiO _x /(FA _{0.83} MA _{0.17}) _{0.95} Cs _{0.05} Pb(I _{0.9} Br _{0.1}) ₃ /PCBM/BCP/Ag | 1.07 | 21.60 | 77.80 | 18.10 | 14 |
| PET/ITO/CuPC/MAPbI ₃ /C ₆₀ /BCP/Ag | 1.10 | 22.65 | 75.00 | 18.68 | 15 |
| PEN/ITO/PEDOT:PSS/PTAA/MAPbI ₃ /PCBM/BCP/Ag | 1.09 | 21.98 | 81.00 | 19.41 | 16 |
| PEN/ITO/NiO _x :PDA/MAPbI ₃ /PCBM/BCP/Ag | 1.04 | 20.78 | 77.40 | 16.76 | 17 |
| PET/ITO/NiO _x /FA _y MA _{1-y} PbI _{3-x} Cl _x /PCBM/BCP/Ag | 1.06 | 22.23 | 73.00 | 17.23 | 18 |
| PET/PEDOT:PSS(PH1000)/PTAA/MAPbI ₃ /C ₆₀ /BCP/Cu/parylene | 0.96 | 22.45 | 79.00 | 17.03 | 19 |
| PET/ITO/NiO _x /Cs _{0.1} FA _{0.7} MA _{0.2} PbI _x Br _{3-x} /PCBM/BCP/Ag | 1.04 | 21.78 | 78.00 | 17.69 | 20 |

References

1. Wu, S., Zhang, J., Qin, M., Li, F., Deng, X., Lu, X., Li, W., Alex, K.Y. (2023). Manipulating Crystallographic Orientation via Cross-Linkable Ligand for Efficient and Stable Perovskite Solar Cells. *Small* 19, 2207189.
2. Gao, D., Li, B., Li, Z., Wu, X., Zhang, S., Zhao, D., Jiang, X., Zhang, C., Wang, Y., Li, Z., Li, N., Xiao, S., Wallace C.H., et al. (2022). Highly Efficient Flexible Perovskite Solar Cells

through Pentylammonium Acetate Modification with Certified Efficiency of 23.35%. *Adv. Mater.* *35*, 2206387.

3. Cheng, H., Liu, C., Zhuang, J., Cao, J., Wang, T., Wong, W., Yan, F. (2022). KBF₄ Additive for Alleviating Microstrain, Improving Crystallinity, and Passivating Defects in Inverted Perovskite Solar Cells. *Adv. Funct. Mater.* *32*, 2204880.

4. Ge, C., Liu, X., Yang, Z., Li, H., Niu, W., Liu, X., Xong, Q. (2021). Thermal Dynamic Self-Healing Supramolecular Dopant Towards Efficient and Stable Flexible Perovskite Solar Cells. *Angew. Chem. Int. Ed.* *61*, e202116602.

5. Choi, J.S., Jang, Y.W., Kim, W., Choi, M., Kang, S.M. (2022). Optically and Mechanically Engineered Anti-Reflective Film for Highly Efficient Rigid and Flexible Perovskite Solar Cells. *Adv. Energy Mater.* *12*, 2201520.

6. Lian, Q., Wang, P., Wang, G., Zhang, X., Huang, Y., Li, D., Mi, G., Shi, R., Amini, A., Zhang, L., Cheng, C. (2022). Doping Free and Amorphous NiO_x Film via UV Irradiation for Efficient Inverted Perovskite Solar Cells. *Adv. Sci.* *9*, 2201543.

7. Liu, S., Guan, X., Xiao, W., Chen, R., Zhou, J., Ren, F., Wang, J., Chen, W., Li, S., Qiu, L., Zhao, Y., Liu, Z., Chen, W. (2022). Effective Passivation with Size-Matched Alkyldiammonium Iodide for High-Performance Inverted Perovskite Solar Cells. *Adv. Funct.* *32*, 2205009.

8. Kang, Y., Li, R., Wang, A., Kang, J.J., Wang, Z., Bi, W., Yang, Y., Song, Y., Dong, Q. (2022). Ionogel-perovskite matrix enabling highly efficient and stable flexible solar cells towards fully-R2R fabrication. *Energy Environ. Sci.* *15*, 3439-3448.

9. Fan, B., Xiong, J., Zhang, Y., Gong, C., Li, F., Meng, X., Hu, X., Yuan, Z., Wang, F., Chen, Y. (2022). A Bionic Interface to Suppress the Coffee-Ring Effect for Reliable and Flexible Perovskite Modules with a Near-90% Yield Rate. *Adv. Mater.* *34*, 2201840.

10. Dou, J., Song, Q., Ma, Y., Wang, H., Yuan, G., Wei, X., Niu, X., Ma, S., Yang, X., Dou, J., Liu, S., Zhou, H., et al. (2023). Improved interfacial adhesion for stable flexible inverted perovskite solar cells. *J. Energy Chem.* *76*, 288-294.

11. Tabakoli, M.M., Tavakoli, R. (2020). All-Vacuum-Processing for Fabrication of Efficient, Large-Scale, and Flexible Inverted Perovskite Solar Cells. *Phys Status Solidi Rapid Res Lett.* *15*, 200049.

12. Wang, Z., Lu, Y., Xu, Z., Hu, J., Chen, Y., Zhang, C., Wang, Y., Guo, F., Mai, Y. (2021). An Embedding 2D/3D Heterostructure Enables High-Performance FA-Alloyed Flexible Perovskite Solar Cells with Efficiency over 20%. *Adv. Sci.* *8*, 2101856.

13. Li, J., Dewi, H.J., Wang, H., Zhao, J., Tiwari, N., Yantara, N., Malinauskas, T., Getautis, V., Savenije, T., Mathews, N., et al. (2021). Co-Evaporated MAPbI₃ with Graded Fermi Levels Enables Highly Performing, Scalable, and Flexible p-i-n Perovskite Solar Cells. *Adv. Funct.* *31*, 2103252.
14. Wang, Z., Rong, X., Wang, L., Wang, W., Lin, H., Lin, X. (2020). Dual Role of Amino-Functionalized Graphene Quantum Dots in NiO_x Films for Efficient Inverted Flexible Perovskite Solar Cells. *ACS Appl. Mater. Interfaces.* *12*, 8342-8350.